Cellulose (2013) 20:873–884
DOI 10.1007/s10570-012-9847-5

ORIGINAL PAPER

# Direct grafting modification of pulp in ionic liquids and self-assembly behavior of the graft copolymers

**Yanzhu Guo · Qili Liu · Hui Chen · Xiaohui Wang · Zuguang Shen · Xuancai Shu · Runcang Sun**

Received: 30 August 2012 / Accepted: 10 December 2012 / Published online: 21 December 2012


**Abstract** In this paper, a novel biodegradable biomass-based amphiphile was prepared by direct grafting copolymerization of dissolved pulp with hydrophobic poly (L-lactide) in ionic liquids BmimCl. The molecular structures of the obtained copolymers were confirmed with $^{1}$H-NMR, $^{13}$C-NMR and 2D HSQC NMR, and their physical properties were studied by TGA and XRD analysis. The self-assembly behaviors of these amphiphilies in aqueous solution was characterized by fluorescence spectrum and their critical micelle concentrations (CMC) were determined to be in the range of 0.326–0.062 mg/mL. TEM observations and DLS analysis revealed that the pulp-derived micelles had spherical and uniform morphology and small diameters (25–125 nm). It was also found that the surface tension of these copolymers solution firstly decreased dramatically with increasing concentration and then approached to a plateau value when the concentration was above their CMC value. MTT assay showed that the pulp-derived amphiphilic micelles exhibited good biocompatibility, which informed that these micelles could be expected to be used in biological regions, especially for the hydrophobic drug delivery system.

**Keywords** Cellulose · Poly(L-lactide) · ROP · Core–shell micelle · Self-assembly

Y. Guo · H. Chen · X. Wang (✉) · Z. Shen · X. Shu · R. Sun
State Key Laboratory of Pulp and Paper Engineering, South China University of Technology, Guangzhou 510640, China
e-mail: fewangxh@scut.edu.cn

Q. Liu
College of Resource and Environment, Henan Institute of Science and Technology, Xinxiang 453003, China

R. Sun
Institute of Biomass Chemistry and Technology, Beijing Forestry University, Beijing 100083, China

## Introduction

Polymeric micelles, generally obtained from self-assembly of amphiphilic polymers composing both hydrophobic and hydrophilic segments, have recently attracted increasingly attentions due to their promising applications in drug delivery (Tao et al. 2012; Wei et al. 2006), volatile molecules encapsulation (Berthier et al. 2011), gene delivery (Hsu et al. 2012; Sawant et al. 2012), bioimaging (Wang et al. 2011c; Yu et al. 2011), sensing for heavy metal ions (Boling et al. 2011; Ma et al. 2011a, b) and trace explosives (Wang et al. 2012), etc. So far, most of the polymeric self-assembly systems are formed from synthetic amphiphilic block/graft copolymers or synthetic hydrophobically modified water-soluble polymers. In the past decade, there has been a growing interest in the self-assemblies from natural polysacchrides and

their derivatives, such as cellulose (Wang et al. 2011a), starch (Yu and Huang 2010), cyclodextrin (Fan et al. 2011), chitosan (Büyüktimkin et al. 2012; Liu et al. 2008; Wang et al. 2011b) and hemicelluloses (Esker et al. 2003; Kaya et al. 2009). In comparison with the synthetic amphiphiles, the natural polysaccharides amphiphiles are more favorable for their inherent renewability, good biocompatibility, biotolerability, and biodegradability properties. Additionally, amphiphiles using natural polysaccharides as raw materials are environmentally friendly, inexpensive to make, and available in large quantities. It can be expected that the amphiphilic natural polysaccharides micelles would have tremendous potential for versatile applications in medicine, pharmacy, sensing, bioimaging and nanoreacting, etc.

Cellulose, as the most abundant and renewable polysaccharides in nature, is an interesting green biomaterial with the potential of replacing the fossil materials (Yan et al. 2009b). Recently, amphiphlic cellulose-based self-assembled nanoparticles have emerged as a new generation of value-added functional nanostructures (Yan et al. 2009a). These amphiphilic celluloses were initially prepared by grafting hydrophobic side chains (*e.g.* long-chain alkyl or ester segments) onto the backbone of cellulose's water-soluble derivatives (*e.g.* hydroxyethyl cellulose, hydroxypropyl cellulose, carboxymethyl cellulose, cellulose sulfate, cationic cellulose, cellulose acetate etc.) (Berthier et al. 2011; Charpentier et al. 1997; Jiang et al. 2011; Kang et al. 2006; Kang et al. 2008; Landoll 1982; Li et al. 2008; Shi and Burt 2003; Song et al. 2011; Sroková et al. 2004; Taylor et al. 1998; Wei and Cheng 2007; Yang et al. 2008). But this procedure had usually been performed in heterogeneous system and resulted in limited degree of hydrophobic substitution, which would restrict their application in entrapping hydrophobic molecules. The amphiphilic cellulose derivatives could also be synthesized by grafting hydrophilic segments (*e.g.* poly(2-hydroxyethyl methacrylate), poly(acrylic acid), poly(poly(ethylene glycol) methyl ether methacrylate etc.) onto the organosoluble cellulose derivatives, for example ethyl cellulose (Kang et al. 2006; Kang et al. 2008; Tan et al. 2010). However, the synthesis process is generally complex by this way. It is highly desirable to realize controlled synthesis of amphiphilic cellulose directly from underivatized cellulose raw material by a straightforward one-pot method. In our past experiments, we have successfully prepared amphiphilic self-associating cellulose-*graft*-long carbon chains (octanoyl, lauroyl, and palmitoyl chlorides) (Guo et al. 2012a) and cellulose-*graft*-poly (L-lactide) (Guo et al. 2012b) with controlled structures from underivatized cellulose by one-pot synthesis in homogeneous system.

However, it should be pointed out that the raw material used in the previous studies was microcrystalline cellulose, which was a refined pure cellulose product. Obviously, the isolation and purification of pure cellulose from the biomass raw materials may involve many chemical procedures, such as delignification and alkali treatment, which could cause environmental pollution and increased expense. Thus it would be more meaningful if the raw biomass residue (bagasse, straw and cornstalk) or the semi-finished biomass products (pulp) could be modified into micelle-forming heteropolysaccharide amphiphiles in the green media of ionic liquids. By that way, the expense and environment burden of making polymeric micelles would be minimized.

In this study, dissolved pulp, a semi-product of wood biomass with cellulose as the major component was used as the raw material to prepare amphiphilic graft copolymers with poly(L-lactide) (PLLA). The cellulose from dissolved pulp has much higher degree of polymerization (DP) than microcrystalline cellulose, which would increase the difficulty in modification but on the other hand provide more insights into the architecture-properties relationship of the cellulose amphiphiles. A green solvent ionic liquid BmimCl capable of dissolving both pulp and hydrophobic monomer was employed to make the graft copolymerization happening in a homogeneous medium. To the best of our knowledge, this is the first report on amphiphilic cellulose nano assemblies developed directly from high molecular weight raw biomass stocks. The aim of this study was to find a way of preparing functional polysaccharide amphiphiles from more feasible biomass residue and provide information for potential value-added applications.

## Experimental and methods

### Materials

The stock of dissolved pulp was supplied by Shandong bohi industry Co., Ltd. Its degree of polymerization

determined by viscometry in cupriethy lenediamine solution at 25 °C was 884. The dissolved pulp was dried in vacuum (60 °C, 100 kPa) for 48 h before use. L-lactide (L-LA, 99.5 % purity) was purchased from Jinan Daigang Biomaterial Co., Ltd (China). 1-butyl-3-methylimidazolium chloride (BmimCl, 99 % purity) derived from Cheng Jie Chemical Co., Ltd (Shanghai, China) was firstly dried in vacuum for 48 h at 50 °C before use. Stannous octanoate ($Sn(Oct)_2$) was provided by Aladdin-reagent Inc. All commercially available solvents and reagents were used without further purification.

## Methods

### *Synthesis and characteristics of pulp-based amphiphilies*

A typical copolymerization procedure was performed as follows. The 3.3 % (w/w) cellulose/BmimCl solution was first prepared by magnetic stirring dissolved pulp in BmimCl at 80 °C for 3 h. Then L-LA monomer and the catalyst $Sn(Oct)_2$ (0.2 wt%) were slowly added into the above solution. The ring opening copolymerization reaction was performed at 110 °C for 8 h under the protection of $N_2$. After cooling to room temperature, the resultant polymer was precipitated with excess anhydrous isopropanol and then the product was purified by stirring in dichloromethane (25 mL) for 72 h. Finally, the purified copolymer was dried at 50 °C in vacuum for 24 h.

$^{1}$H-NMR and $^{13}$C-NMR were performed on a Bruker AV-III 400 M spectrometer (Germany) with a standard probe at room temperature. All spectra of the graft copolymers were acquired in the DMSO-$d_6$ solvent with tetramethysilane (TMS) as internal standard. The size-exclusion chromatography and multi-angle laser light scattering (PL aquagel-OH 40) analyses were used to determine the molecular weights of copolymers. A dual-detector system, consisting of a MALLS device and an interferometric refractometer was used. The concentration of each sample was kept constant at 5 mg/mL and the ultra pure water filtered through 0.22 μm membrane was used as the eluent at a flow rate of 0.5 mL/min. The MALLS detector was operated at a laser wavelength of 690 nm. The dn/dc value of copolymers was 0.1341 (Table 1). X-ray diffraction (XRD) patterns of the powder samples were obtained on a D/max-IIIA X-ray diffractometer with a Cu Kα radiation source (40 kV, 40 mA). Samples were exposed at a scanning rate of $2\theta = 5°–45°$. The thermogravimetric analysis (TGA) (TGA Q500, TA, USA) was carried out in an aluminum crucible by heating to 600 °C at a heating rate of 10 °C $min^{-1}$ while the apparatus was continually flushed with a nitrogen flow of 30 mL $min^{-1}$.

### *Self-assembly behavior of pulp-based amphiphilies*

The value of CMC was determined by a pyrene fluorescence probe method using fluorescence spectrometer. Typically, the pyrene methanol solution ($6.0 \times 10^{-4}$ M) was added into the test tubes and evaporated under a stream of nitrogen gas to remove the solvents. Then, the water solutions of cellulose-*g*-PLLA copolymers were added into the test tubes. The final concentration of pyrene in a sample solution was controlled at $6.0 \times 10^{-6}$ M, which was close to the maximum solubility of pyrene in water at 25 °C. The mixtures were sonicated for 30 min in an ultrasonic bath and shaken in a shaking bath for 1 h at room temperature. The emission spectra of pyrene labeled solution were recorded on a fluorescence spectrometer (Jobin–Yvon Fluorolog Tau-3 system). The probe was excited at 339 nm, and the emission spectra were recorded in the range of 350–500 nm at an integration time of 1.0 s. The excitation and emission slit openings were 10 and 2.5 nm, respectively.

The average hydrodynamic diameters of pulp-based amphiphilies micelles were measured by dynamic light scattering (DLS) using a Malvern 90 Plus particle size analyzer (Marlvern Instruments, Malvern, UK).

The morphology and size distribution were observed by a transmission electron microscopy (TEM, JEM-2100, Japan). The sample solution was dropped onto the carbon-coated 300 mesh copper grid and air-dried, followed by the application of phosphotungstic acid (2 %, w/w) negative staining for 3 min.

### *Surface tension*

The surface tension of the pulp-based amphiphiles' aqueous solutions at the air–water interface was measured by the Wilhelmy plate method with dynamic contact angle analyzer (Dataphysics DCAT21, Germany) at 30 °C. The concentrations of copolymers

**Table 1** Results of homogeneous graft polymerization of PLLA onto cellulose in BmimCl

| Sample | AGU/L-LA (mol ratio) | $DP^{a}_{PLLA}$ | $MS^{a}$ | $DS^{a}$ | $W^{a}_{PLLA}$ (%) | $M^{b}_{w}$ | $M_w/M^{b}_{n}$ | Solubility | |
|---|---|---|---|---|---|---|---|---|---|
| | | | | | | | | DMSO | $H_2O$ |
| 1 | 1:2 | 1.78 | 1.30 | 0.73 | 36.62 | 88,620 | 1.24 | +++ | +++ |
| 2 | 1:3 | 1.86 | 1.68 | 0.90 | 42.75 | 99,800 | 1.60 | +++ | +++ |
| 3 | 1:4 | 2.09 | 2.25 | 1.08 | 50.00 | 105,100 | 1.64 | +++ | +++ |
| 4 | 1:5 | 2.02 | 2.38 | 1.18 | 51.40 | 108,620 | 1.78 | +++ | +++ |
| 5 | 1:6 | 2.21 | 3.00 | 1.36 | 57.14 | 115,240 | 1.29 | +++ | +++ |
| 6 | 1:8 | 2.32 | 3.53 | 1.52 | 61.07 | 123,480 | 1.32 | +++ | +++ |

[a] The DPPLLA, MS, DS and WPPLA values were determined by $^{1}$H-NMR spectroscopy

[b] Determined by GPC analysis

+++ Dissolving

were varied from $1 \times 10^{-3}$ to 5 mg/mL. All measurements were performed for at least $10^4$ s in order to monitor the slow equilibration of the adsorption layers.

*Cytotoxicity test*

The in vitro cytotoxicity of the pulp-based amphiphilies on 3T3 mouse fibroblasts was evaluated by the standard methylthiazoltetrazolium (MTT) assay. Live 3T3 mouse fibroblasts without any treatment were used as a control with no exogenous cytotoxicity. For cytotoxicity assay, 3T3 mouse fibroblasts were seeded in a 96-well plate at an initial density of $1 \times 10^4$ cells/well in 100 μL of Dulbecco's modified Eagle medium (DMEM) supplemented with 10 % fetal bovine serum (FBS) and cultured for 24 h in incubator (37 °C, 5 %$CO_2$). After that the culture medium was changed to 100 μL of DMEM containing cellulose-*g*-PLLA copolymers with particular concentrations and the mixture was further incubated for 24 h. Then DMEM with copolymers was replaced by fresh DMEM and 10 μL of MTT solution was added to the fibroblasts. After incubation for 4 h, 100 μL of DMSO was added and shaken at room temperature. The optical density (OD) was measured at 570 nm with a microplate reader (Multiskan Spectrum, Thermo Scientific, Finland). The relative cell viability was calculated by the following equation: cell viability = ($OD_{treated}$/$OD_{control}$) × 100 %, where $OD_{control}$ was obtained in the absence of copolymer and $OD_{treated}$ was obtained in the presence of copolymer.

## Results and discussion

### Synthesis and characterization of pulp-based amphiphiles

The pulp-based amphiphiles were synthesized via a ring-opening copolymerization (ROP) of L-LA onto the dissolved pulp substrate. Since the main component of dissolved pulp is cellulose, we can refer these pulp-based amphiphiles as the cellulose-based amphiphiles. The synthesis route was elucidated in Scheme 1a. As shown in Scheme 1a, $Sn(Oct)_2$ was utilized as the catalyst for the ROP of L-LA, while the hydroxyl groups in the backbone of cellulose functioned as the initiator. The solvent used in this experiment was ionic liquid BmimCl, which was a recyclable green solvent for biomass (Heinze et al. 2005). Moreover, the hydrophobic monomer L-LA and catalyst could be also dissolved in BmimCl, thus the ROP reaction was able to be carried out in a homogeneous system.

The obtained cellulose-*g*-PLLA copolymers were characterized by $^{1}$H-NMR, $^{13}$C-NMR and 2D HSQC NMR spectra to prove their molecular structure. The results of $^{13}$C-NMR analysis are shown in Fig. 1. Compared with the dissolved pulp raw materials, a number of new signals contributed by the grafted side chains appear in the spectrum of cellulose-*g*-PLLA. For example, the new peaks appearing at 68.4, 66.3, 21.1, and 17.3 ppm are ascribed to b1, b2, d2 and d1 (indexed in Fig. 1) of the PLLA side chains, respectively (Gong et al. 2006; Hiltunen et al. 1996). The two peaks at chemical shifts of 174.1 and 169.8 ppm are attributed to the carbonyl carbons of the repeating and

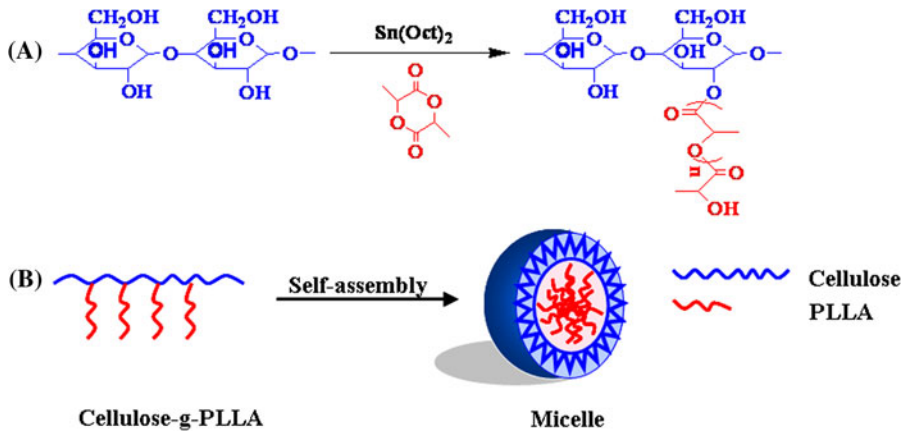


**Scheme. 1** **a** Synthesis of cellulose-g-PLLA copolymers in Ionic Liquid BmimCl. **b** The preparation of nano-sized micelles from cellulose-g-PLLA copolymers in aqueous water

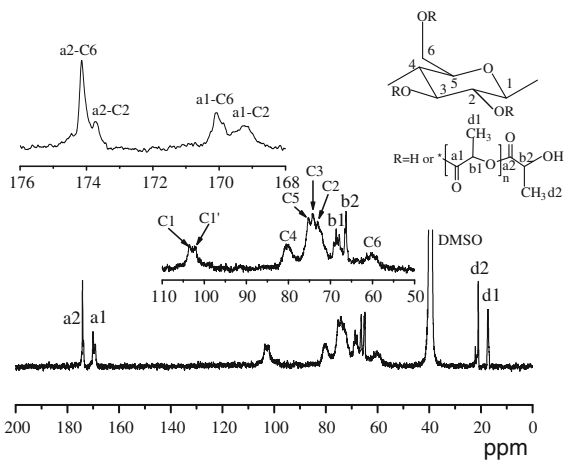


**Fig. 1** $^{13}$C-NMR (DMSO-$d_6$) Spectrum of Cellulose-g-PLLA copolymers (Sample 4)

ending unit of PLLA side chains, respectively. Furthermore, in the magnified spectrum from 168 to 176 ppm, there are two peaks (174.1 and 173.7 ppm) belonging to the carbonyl carbons of a2 that can be assigned to the O-lactyl carbonyl carbons in C6 and C2 positions, respectively. The carbons of the cellulose backbone appeare at 103.0, 70.9–76.4, 79.9, and 60.1 ppm corresponding to C1, C2, 3, 5, C4 and C6 in anhydrous glucose units (AGU), respectively. The chemical shifts of C1 (103.0 ppm) and C1' (99.6 ppm) correspond to the C1 carbons adjacent to C2 bearing un-substituted and substituted hydroxyl groups, respectively. Accordingly, C6 (60.1 ppm) and C6' (63.7 ppm) are ascribed to the C6 carbons bearing un-substituted and substituted hydroxyl groups, respectively. These results indicated that the hydroxyl groups of AGU in native cellulose were partially substituted.

More specific information about cellulose-*g*-PLLA copolymer (Sample 4) was obtained by 2D HSQC NMR spectra (Fig. 2) studies. Obviously, the marked $^{1}$H/$^{13}$C cross-peaks in the HSQC spectra at δ1.29/20.93, 1.45/17.13, 4.19/66.25 and 5.11/68.47 ppm confirmed the structural element of PLLA chains in cellulose-*g*-PLLA copolymer, which were attributed to the terminal $CH_3$, internal $CH_3$, terminal CH and internal CH groups, respectively. The cross-peaks at δ3.08/72.91, 3.35/80.20, 3.36/74.50, 4.41/102.70 ppm are assigned to the typical groups of AGU in cellulose-*g*-PLLA copolymer. The HSQC spectra enable us to assign the signals of cellulose-*g*-PLLA copolymer more accurately.

Figure 3 gives a typical $^{1}$H-NMR spectrum of the resulting graft copolymer. According to Fig. 3, new strong signals at 1.45 and 1.29 ppm corresponding to the internal and terminal methyl protons ($H_b$ and $H_{b'}$) of PLLA side chain and the peaks at 5.09 and 4.20 ppm assigned to the internal and terminal methine protons ($H_a$ and $H_{a'}$) of PLLA side chain, respectively, appear in the spectrum of cellulose-*g*-PLLA. The protons of the glucose unit appear at 4.66, 3.77, 3.55 and 3.05 ppm which belong to $H_1$, $H_{3,\ 6,\ 5}$, $H_2$ and $H_4$ in the AGU units of cellulose, respectively. Meanwhile, the signals at 5.46, 5.40 and 4.31 ppm are ascribed to the H-2, H-3 and H-6 protons of residual hydroxyl in cellulose. Based on the above peak assignments, the microstructure of cellulose-*g*-PLLA

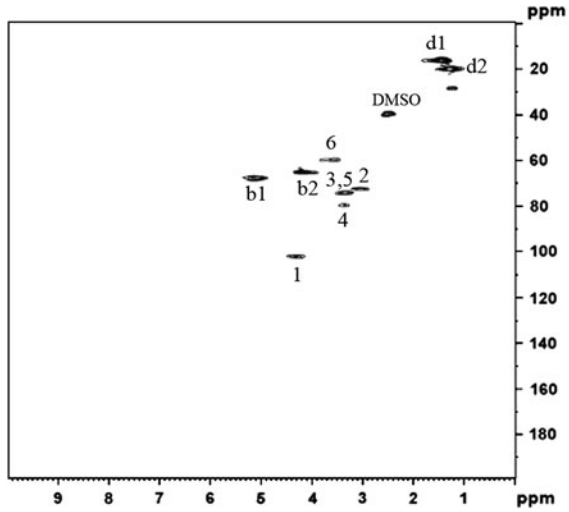


**Fig. 2** Typical two-dimensional HSQC spectra (DMSO-$d_6$) of cellulose-*g*-PLLA copolymers (Sample 4)

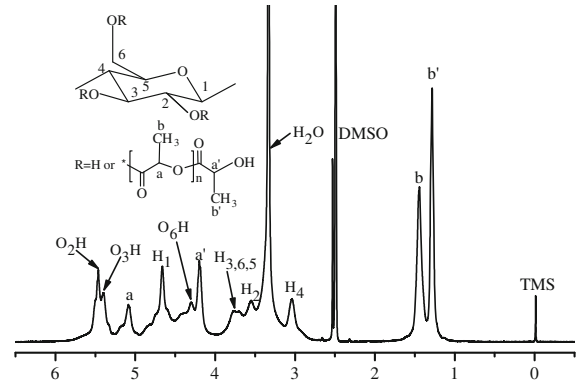


**Fig. 3** $^1$H-NMR (DMSO-$d_6$) Spectrum of Cellulose-*g*-PLLA copolymers (Sample 4)

copolymers can be analyzed in detail through calculations with the peak intensity in their $^1$H-NMR spectra as following:

$$\mathrm{MS} = \frac{\text{lactyl units}}{\text{anhydroglucose units}} = \frac{I_{(b+b')}/3}{I_{(O2H+O3H+O6H)}/3} \quad (1)$$

$$\mathrm{DS} = \frac{\text{terminal lactyl units}}{\text{anhydroglucose units}} = \frac{I_{b'}/3}{I_{(O2H+O3H+O6H)}/3} \quad (2)$$

$$\mathrm{DP_{PLLA}} = \frac{\mathrm{MS}}{\mathrm{DS}} = \frac{\mathrm{IA_b}}{\mathrm{IA_{b'}}} + 1 \quad (3)$$

$$\mathrm{W_{PLLA}} = \frac{72\mathrm{MS}}{162 + 72\mathrm{MS}} \times 100\ \% \quad (4)$$

Where $\mathrm{DP_{PLLA}}$, DS, MS and $\mathrm{W_{PLLA}}$ delegate the degree of polymerization of PPLA side chains, degree of substitution of copolymer, the molar of substitution of copolymer, the weight content of PPLA side chains in copolymer, respectively.

In order to investigate the effect of molar feed ratio of cellulose with L-LA on the structure parameters of cellulose-*g*-PLLA copolymers, a series of reactions with varying molar feed ratio of cellulose with L-LA were carried out. Table 1 showed the resultant $\mathrm{DP_{PPLA}}$, DS, MS and $\mathrm{W_{PPLA}}$ values of the copolymers as a function of the different feeding amount of monomer L-LA. According to the results, it can be found that the values of $\mathrm{DP_{PPLA}}$, DS, MS and $\mathrm{W_{PPLA}}$ are increased when the dosage of L-LA monomer is increased from 2:1 to 8:1 (based on the molar ratio of L-LA to AGU). With maximum dosage of L-LA monomer in the copolymerization, the values of $\mathrm{DP_{PPLA}}$, DS, MS and $\mathrm{W_{PPLA}}$ of the graft copolymer reach 2.32, 3.53, 1.52 and 61.07 %, respectively. If the degree of hydrophobic modification is too high, the copolymers would be hardly soluble in aqueous solution (Guo et al. 2012b), which is not preferred in this study, thus the copolymers with even higher grafting ratios were not prepared.

## Physical properties of the modified pulp derivatives

XRD and TGA spectrometry were employed to study the physical properties of cellulose and its copolymer derivatives. XRD was conducted for cellulose and cellulose-*g*-PLLA with different DS values of PLLA (samples 2, 4 and 6) to evaluate their crystallization behaviors (Fig. 4). As shown in Fig. 4, three diffraction peaks at 2θ of 15.3, 22.6 and 34.7° corresponding to the typical diffraction patterns of cellulose type I (Guo et al. 2012b) are observed in the X-ray diffraction pattern of dissolved pulp. In the X-ray diffraction pattern of the regenerated cellulose after being dissolved in BmimCl and subsequently precipitated in isopropanol, there appear one broad peak at $2\theta = 20.3°$ and one small reflection signal at 35.1° indicating the appearance of cellulose type II (Gindl and Keckes 2005). The X-ray diffraction patterns of cellulose-*g*-PLLA copolymers show more prominent cellulose II structure with only one broad signal peaking at 2θ of about 20°. These results demonstrate

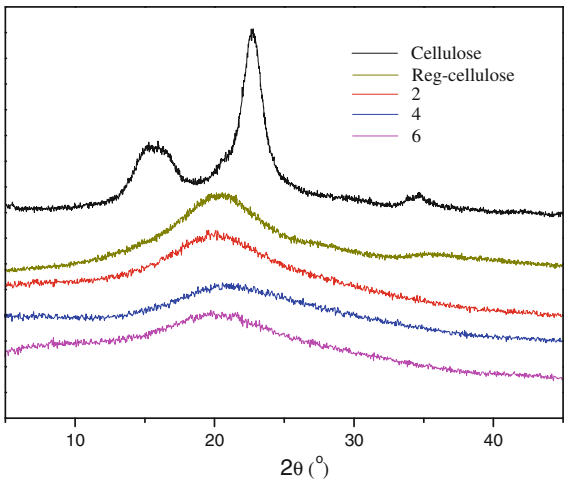


**Fig. 4** The XRD patterns of cellulose, regenerated cellulose and cellulose-*g*-PLLA copolymers

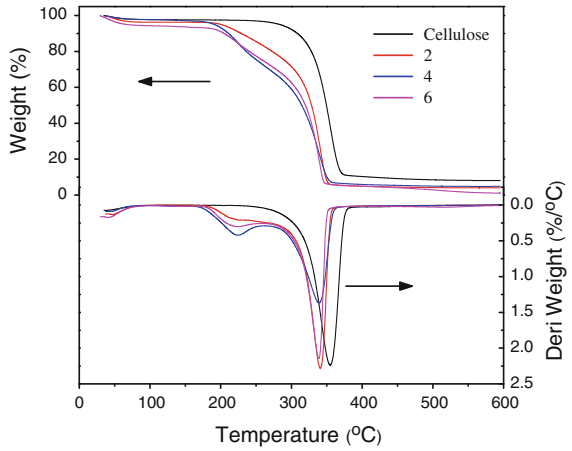


**Fig. 5** TG and DTG curves of cellulose and cellulose-*g*-PLLA copolymers

that the original crystallization of cellulose was destroyed by the dissolution and precipitation process in BmimCl and the introduction of PLLA group to the cellulose main chain.

The TGA curves of cellulose and cellulose-*g*-PLLA copolymers are shown in Fig. 5. It can be seen that the thermal stability of cellulose is decreased after grafting PLLA copolymer. Cellulose-*g*-PLLA copolymers have two decomposition stages and two maximum decomposition temperatures ($T_{max}$), while cellulose has only one decomposition stage and one maximum decomposition temperature. $T_{max1}$ of the cellulose-*g*-PLLA copolymers corresponds to the scission of the PLLA linkage in the cellulose backbone then the decomposition of the PLLA grafts, and $T_{max2}$ is ascribed to the decomposition of cellulose backbone. However, $T_{max2}$ of cellulose-*g*-PLLA is still lower than that of cellulose confirming the fact that hydrogen bonds of cellulose had been partially destroyed by the introduction of PLLA. Similar phenomenon was reported by (Yan et al. 2009a).

## Physicochemical properties of pulp-based amphiphilies micelles

With both of the hydrophobic PLLA segments and hydrophilic cellulose backbone, the synthesized cellulose-*g*-PLLA copolymers exhibited self-associating properties in water and were able to self-assemble into micelles when their concentration approached a certain level. In general, the hydrophobic PLLA segments self-assemble into the hydrophobic core, while the hydrophilic cellulose segments are pushed into water phase surrounding the core, as shown in Scheme 1 (B). The fluorescence probe method using pyrene as the probe molecule was employed to examine the critical micelle concentration (CMC) values of cellulose-*g*-PLLA copolymers. Pyrene is a poorly soluble fluorescent probe with very sensitive photoluminescence properties to the polarity of environment. Once the hydrophobic association occurs in aqueous solution, pyrene would be concentrated at the hydrophobic regions, resulting in the change of its photophysical character. Therefore, pyrene has been widely used to monitor the association of amphiphilic copolymers in aqueous solution (Winnik and Regismond 1996). Fig. 6 shows the fluorescence intensity ratio of $I_1/I_3$ of pyrene in respond to the log concentration of cellulose-*g*-PLLA copolymers. When the concentration of cellulose-*g*-PLLA copolymers was very low, the value of $I_1/I_3$ was kept high in a hydrophilic environment and did not change significantly with the increasing concentration. With further increase of the copolymers' concentration, the $I_1/I_3$ values decreased sharply. This indicates that the cellulose-*g*-PLLA copolymers start to associate due to the hydrophobic interaction and the pyrene probe has transferred into the hydrophobic regions. The concentration value at the inflection point is the critical micelle concentration of the cellulose-*g*-PLLA copolymers. According to the plot curves in Fig. 6, it

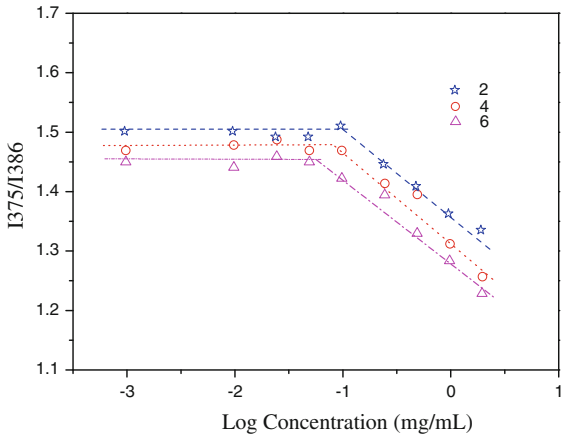


**Fig. 6** The Intensity ratio ($I_{375}/I_{386}$) of the pyrene emission spectra versus the log concentration of cellulose-*g*-PLLA coplolymers

can be determined that the CMC of cellulose-*g*-PLLA samples 2, 4, and 6 are about 0.122, 0.078, and 0.062 mg/mL, respectively. The CMC values for samples 1, 3, and 5 were also determined by this method and listed in Table 2 as 0.326, 0.112, and 0.071 mg/mL, respectively. Obviously, the CMC values of the amphiphilic copolymers decrease with increasing PLLA contents in copolymers. This is because the hydrophobic interaction between the PLLA segments is enhanced with the increasing graft ratio of PLLA. Therefore, micelles are able to form at low concentration. The same trend was also observed in other literature (Zhang et al. 2012) .

The self-assembly behaviors of cellulose-*g*-PLLA copolymers were further studied by exploring their surface tensions in water in respond to the concentrations. The surface tension will decrease greatly when the amphiphilic copolymers self-assemble in the water/air interface with the hydrophobic segment stretching outside and hydrophilic segment sticking inside. When the interface is completely transformed to hydrophobic, the amphiphilic cellulose copolymers will begin to self-assemble into micelles in aqueous water, wherein the surface tension will achieve a minimal value. Figure 7 shows the surface tension of cellulose-*g*-PLLA copolymer solutions as a function of concentration. It can be found that the surface tension values of cellulose-*g*-PLLA copolymer solutions firstly decrease and subsequently approach a plateau value with continuing increase of

**Table 2** The CMC values and average sizes of cellulose-*g*-PLLA micelles

| Sample | CMC (mg/ml) | | Particle size (nm) | PDI |
|---|---|---|---|---|
| | a | b | | |
| 1 | 0.326 | – | 116.96 | 0.428 |
| 2 | 0.122 | 0.116 | 93.20 | 0.450 |
| 3 | 0.112 | – | 76.40 | 0.404 |
| 4 | 0.078 | 0.060 | 61.94 | 0.342 |
| 5 | 0.071 | – | 40.95 | 0.430 |
| 6 | 0.062 | 0.040 | 25.04 | 0.417 |

[a] Determined by fluorescence spectra

[b] Determined by surface tension

concentration. It is evident that cellulose-*g*-PLLA copolymers exhibited significant surface activities. The critical micelle concentration can also be determined from the breakpoint surface tension in respond to concentration. The CMC values ($\gamma_{CMC}$) of cellulose-*g*-PLLA samples 2, 4, and 6 determined by surface tension analysis are about 0.116, 0.060, 0.040 mg/mL, respectively, which are similar to those obtained from fluorescence spectra. The surface tension values at CMC ($\gamma_{CMC}$) for samples 2, 4 and 6 as shown in Table 2 are 58.91, 52.39 and 50.65 mN/m, respectively. It can be deduced that fhe $\gamma_{CMC}$ values decrease with increasing PLLA content in the copolymers. This suggests that more hydrophobic PLLA grafted in the cellulose backbone would result in higher surface activity (Jiang et al. 2011).

Cellulose-*g*-PLLA micelles were prepared by dispersing copolymers in ultra pure water with probe-type ultrasonic treatment. Table 2 and Fig. 8 summarize the properties and morphology of cellulose-*g*-PLLA micelles.

The morphology and size distribution of the micelles self-assembled from of cellulose-*g*-PLLA copolymer (sample 4) were analyzed by TEM (Fig. 8a) and DLS measurement (Fig. 8b). The concentration of the sample solution for observation was controlled at 0.25 mg/mL, which was about three times higher than CMC, in order to ensure the formation of self-assembled polymeric micelles. The TEM images reveal that amphiphilic cellulose copolymers could self-assemble into spherical micelles with the diameters ranging from 20 nm to 60 nm in water. DLS measurement results show a narrow size distribution of self-assembled micelles with the

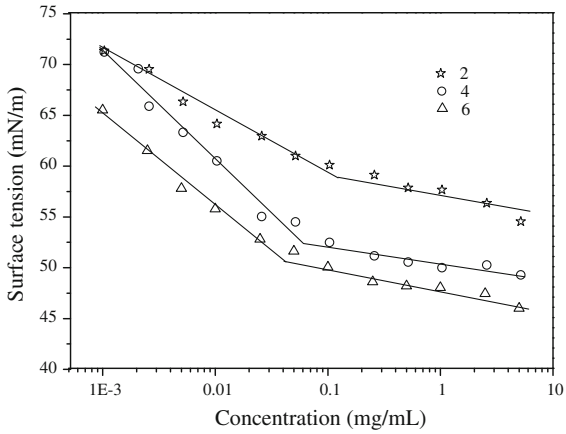


**Fig. 7** The concentration dependence of surface tension of cellulose-*g*-PLLA coplolymers (samples 2, 4 and 6)

hydrodynamic diameters varied in the range of 30–120 nm. The average diameter of sample 4 micelles is 62 nm. The difference in micelle size determined by TEM and DLS is because the latter measures the hydrodynamic diameter of micelles in solvated state, while the former one presents the morphological size in solid and dry state. It is assumed that the PLLA moieties are tightly held in the micelle core, while the cellulose moieties are loosely packed outside. The loose outer layer tends to shrink and become compact while the micelles are conversion to solid state. (Bajgai et al. 2009).

The average sizes of cellulose-*g*-PLLA micelles with different graft ratio of PLLA were calculated to explore the effects of copolymers structure on their self-assembled nanostructures. As shown in Table 2, the average sizes of prepared micelles measured by DLS are in the range of 25–120 nm, and the micelle sizes reduce with increasing the graft ratio of hydrophobic PLLA groups. This is because that the conformation of cellulose-*g*-PLLA copolymers is affected by the hydrophobic interaction of PLLA groups. The cellulose-*g*-PLLA copolymers with higher graft ratio of PLLA would have stronger hydrophobic interaction, and thus are able to self-assemble into micelles with denser hydrophobic cores as compared with those having lower graft ratio of PLLA groups. Therefore, higher graft ratio of hydrophobic PLLA groups in the copolymers results in smaller micelle diameter.

The self-assembly behaviors of the cellulose-based amphiphiles were also affected by the molecular

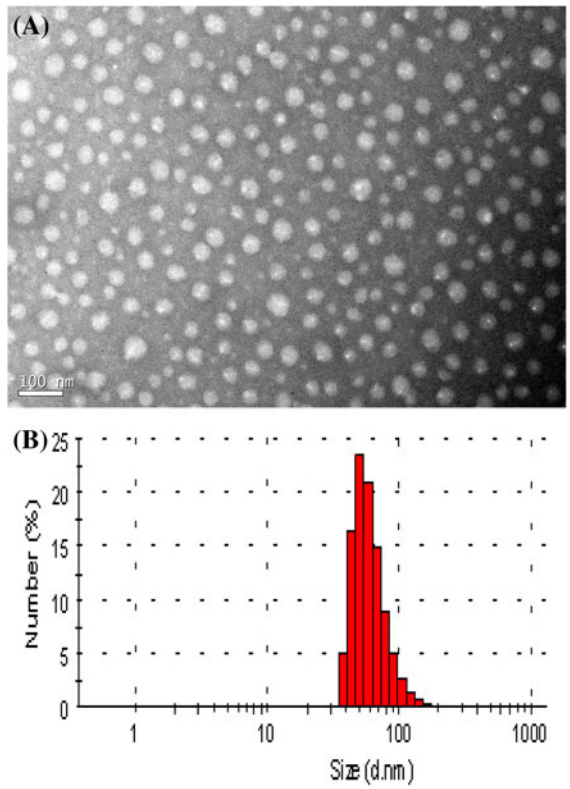


**Fig. 8** TEM micropicture (**a**) and size distribution (**b**) of cellulose-*g*-PLLA micelles for Sample 4

properties of the starting raw materials. In the previous studies, we had prepared and characterized the cellulose-*g*-PLLA nanomicelles from microcrystalline cellulose (MCC) with DP of 200. Their CMC values and particle sizes were identified in the range of 0.13–0.43 mg/mL and 13.27–51.35 nm, respectively (Guo et al. 2012b). Comparing with the amphiphiles from MCC, the cellulose-*g*-PLLA amphiphiles prepared from dissolving pulp (DP = 884) in this paper are more advantageous and stable for their lower CMC values. For example, the CMC value of the sample from MCC with a PLLA's DS of 1.37 was determined to be 0.15 mg/mL, while that of the dissolving pulp sample with similar PLLA's DS (1.36) was only 0.071 mg/mL. These results indicate the self-assembly behaviors of the cellulose amphiphiles are not only determined by the hydrophobic segments content of the amphiphiles, but also determined by the molecular weight of the starting materials. The amphiphilic cellulose nanomicelles prepared from high molecular weight raw materials exhibited higher stability against

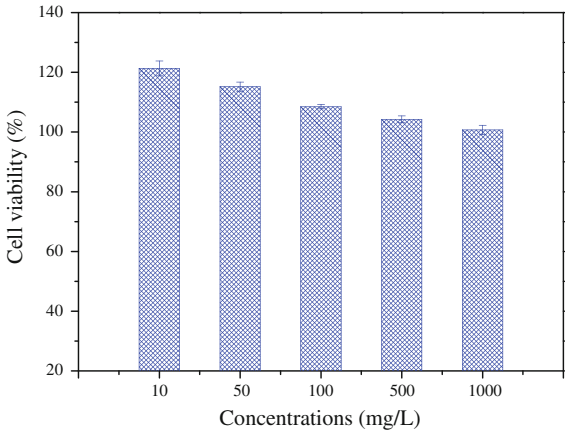


**Fig. 9** Cytotoxicity studies of cellulose-*g*-PLLA copolymers with different concentrations

dilution. On the other hand, however, high molecular weight starting materials may also result in larger nanomicelle size. It was observed that the particle sizes of nanomicelles from dissolving pulp were higher than those from MCC with similar graft ratio of PLLA side chains.

### Cytotoxicity study of pulp-based amphiphilies micelles

It has been well established that the polymeric micelles have the potential of loading functional hydrophobic molecules, such as hydrophobic anticancer drugs, fluorescent probes, diagnosis agents etc., due to the micro-extraction effect of their hydrophobic cores and being applied in nanoscale biosensors, biocatalysts and bioimaging (Boling et al. 2011; Liu et al. 2005). As regard to the applications in biological region, the biocompatibility and cytotoxicity of micelles are very important factors to consider. In this study, the cytotoxicity study on the proliferation of 3T3 fibroblast was carried out to investigate the preliminary biocompatibility of resulting cellulose-*g*-PLLA copolymers. The effect of the copolymer concentration on the proliferation of 3T3 fibroblast was studied (Fig. 9). The results showed that no apparent inhibition effect caused by the copolymer when the concentration of it was below 1,000 mg/L, which was preponderant in comparison of 700 mg/L in the similar materials (Dong et al. 2008). It indicates that the cellulose-*g*-PLLA nanomicelles prepared in this study have good biocompatibility.

## Conclusions

In this paper, ring-opening copolymerization of L-LA onto pulp cellulose backbone was performed in homogeneous ionic liquids system and obtained amphiphilic graft copolymers, cellulose-*g*-PLLA. The analysis of $^{1}$H-NMR and $^{13}$C-NMR confirmed the successful synthesis. The physical properties of the copolymers were studied by TGA and XRD analysis. It was found increase in the molar ratio of L-LA to cellulose in feed could modify the structural parameters of the obtained copolymers. The amphiphilic cellulose-*g*-PLLA copolymers could self-assemble into the naonsized micelles with core/shell structure, in which the PLLA segments formed the hydrophobic inner core and cellulose comprised the outer hydrophilic shell. TEM observations and DLS analysis revealed that these polymeric micelles were spherical and uniform in morphology with diameters in the range of 25–120 nm Their CMC values were determined to be in the range of 0.326–0.062 mg/mL, and tended to decrease with increasing graft ratio of PLLA. The surface tension of cellulose-*g*-PLLA copolymers solution firstly decreased dramatically with increasing concentration and then approached to a plateau value when the concentration was above the CMC value of cellulose-*g*-PLLA copolymers. The cytotoxicity study showed that the cellulose-*g*-PLLA copolymers have good compatibility, which informed that these pulp-derived micelles could be expected to be used in biological regions.

**Acknowledgments** This work was supported by the grants from the National Natural Science Foundation of China (51103046) and Ministry of Science and Technology, 973 projects (2010CB732201, 2010CB732204).

## References

Bajgai MP, Parajuli DC, Ko JA, Kang HK, Khil MS, Kim HY (2009) Synthesis, characterization and aqueous dispersion of dextran-g-poly(1, 4-dioxan-2-one) copolymers. Carbohydr Polym 78(4):833–840

Berthier DL, Herrmann A, Ouali L (2011) Synthesis of hydroxypropyl cellulose derivatives modified with amphiphilic diblock copolymer side-chains for the slow release of volatile molecules. Polym Chem 2(9):2093–2101

Büyüktimkin B, Wang Q, Kiptoo P, Stewart JM, Berkland C, Siahaan TJ (2012) Vaccine-like controlled-release delivery of an immunomodulating peptide to treat experimental autoimmune encephalomyelitis. Mol Pharm 9:979–985

Charpentier D, Mocanu G, Carpov A, Chapelle S, Merle L, Müller G (1997) New hydrophobically modified carboxymethylcellulose derivatives. Carbohydr Polym 33(2–3): 177–186

Dong HQ, Xu Q, Li YY, Mo SB, Cai SJ, Liu LJ (2008) The synthesis of biodegradable graft copolymer cellulose-graft-poly (L-lactide) and the study of its controlled drug release. Colloids Surf B Biointerfaces 66(1):26–33

Esker A, Becker U, Jamin S, Beppu S, Renneckar S, Glasser W (2003) Self-assembly behavior of some co-and heteropolysaccharides related to hemicelluloses. In hemicelluloses science and technology, American chemical society 864:198–219

Fan MM, Xi Z, Li BJ, Sun X, Zhang S (2011) Supramolecular assembly of cyclodextrin-based nanospheres for gene delivery. J Control Release 152(Supplement 1):141–142

Gindl W, Keckes J (2005) All-cellulose nanocomposite. Polymer 46(23):10221–10225

Gong Q, Wang L-Q, Tu K (2006) In situ polymerization of starch with lactic acid in aqueous solution and the microstructure characterization. Carbohydr Polym 64:501–509

Guo YZ, Wang XH, Li D, Du H, Wang XY, Sun RC (2012a) Synthesis and characterization of hydrophobic long-chain fatty acylated cellulose and its self-assembled nanoparticles. Polym Bull 69(4):389–403

Guo YZ, Wang XH, Shu XC, Shen ZG, Sun RC (2012b) Self-assembly and paclitaxel loading capacity of cellulose-graft-poly (lactide) nanomicelles. J Agric Food Chem 60(15):3900–3908

Heinze T, Schwikal K, Barthel S (2005) Ionic liquids as reaction medium in cellulose functionalization. Macromol Biosci 5:520–525

Hiltunen K, Härkönen M, Seppälä JV, Väänänen T (1996) Synthesis and characterization of lactic acid based telechelic prepolymers. Macromolecules 29:8677–8682

Hsu SH, Ho TT, Tseng TC (2012) Nanoparticle uptake and gene transfer efficiency for MSCs on chitosan and chitosan-hyaluronan substrates. Biomaterials 33(14):3639–3650

Jiang C, Wang XL, Sun PD, Yang C (2011) Synthesis and solution behavior of poly(ε-caprolactone) grafted hydroxyethyl cellulose copolymers. Int J Biol Macromol 48(1): 210–214

Kang HL, Liu WY, He BQ, Shen DW, Ma L, Huang Y (2006) Synthesis of amphiphilic ethyl cellulose grafting poly(-acrylic acid) copolymers and their self-assembly morphologies in water. Polymer 47(23):7927–7934

Kang HL, Liu WY, Liu RG, Huang Y (2008) A novel, amphiphilic ethyl cellulose grafting copolymer with poly(2-hydroxyethyl methacrylate) side chains and its micellization. Macromol Chem Phys 209(4):424–430

Kaya A, Drazenovich DA, Glasser WG, Heinze T, Esker A (2009) Hydroxypropyl xylan self-assembly at air/water and water/cellulose interfaces. In model cellulosic surfaces, American chemical society 1019:173–191

Landoll LM (1982) Nonionic polymer surfactants. J Polym Sci: Polym Chem Edition 20(2):443–455

Li YX, Liu RG, Liu WY, Kang HL, Wu M, Huang Y (2008) Synthesis, self-assembly, and thermosensitive properties of ethyl cellulose-g-P(PEGMA) amphiphilic copolymers. J Polym Sci, Part A: Polym Chem 46(20):6907–6915

Liu CG, Desai KGH, Chen XG, Park HJ (2005) Preparation and characterization of nanoparticles containing trypsin based on hydrophobically modified chitosan. J Agric Food Chem 53(5):1728–1733

Liu KH, Chen SY, Liu DM, Liu TY (2008) Self-assembled hollow nanocapsule from amphiphatic carboxymethyl-hexanoyl chitosan as drug carrier. Macromolecules 41(17): 6511–6516

Ma BL, Xu MY, Zeng F, Huang LF, Wu SZ (2011a) Micelle nanoparticles for FRET-based ratiometric sensing of mercury ions in water, biological fluids and living cells. Nanotechnology 22(6):065501

Ma C, Zeng F, Huang LF, Wu SZ (2011b) FRET-based ratiometric detection system for mercury ions in water with polymeric particles as scaffolds. J Physic Chem B 115(5): 874–882

Sawant RR, Sriraman SK, Navarro G, Biswas S, Dalvi RA, Torchilin VP (2012) Polyethyleneimine-lipid conjugate-based pH-sensitive micellar carrier for gene delivery. Biomaterials

Shi RW, Burt HM (2003) Synthesis and characterization of amphiphilic hydroxypropylcellulose-graft-poly (ε-caprolactone). J Appl Polym Sci 89(3):718–727

Song YB, Zhang LZ, Gan WP, Zhou JP, Zhang LN (2011) Self-assembled micelles based on hydrophobically modified quaternized cellulose for drug delivery. Colloids Surf B Biointerfaces 83(2):313–320

Sroková I, Tomanová V, Ebringerová A, Malovíková A, Heinze T (2004) Water-soluble amphiphilic O-(carboxymethyl) cellulose derivatives-synthesis and properties. Macromol Mater Eng 289(1):63–69

Tan JJ, Li YX, Liu RG, Kang HL, Wang DQ, Ma L, Liu WY, Wu M, Huang Y (2010) Micellization and sustained drug release behavior of EC-g-PPEGMA amphiphilic copolymers. Carbohydr Polym 81(2):213–218

Tao YH, Han JF, Dou HY (2012) Paclitaxel-loaded tocopheryl succinate-conjugated chitosan oligosaccharide nanoparticles for synergistic chemotherapy. J Mater Chem 22(18): 8930–8937

Wang DQ, Tan JJ, Kang HL, Ma L, Jin X, Liu RG, Huang Y (2011a) Synthesis, self-assembly and drug release behaviors of pH-responsive copolymers ethyl cellulose-graft-PDEAEMA through ATRP. Carbohydr Polym 84(1): 195–202

Wang Q, Jamal S, Detamore MS, Berkland C (2011b) PLGA-chitosan/PLGA-alginate nanoparticle blends as biodegradable colloidal gels for seeding human umbilical cord mesenchymal stem cells. J Biom Mater Res A 96A: 520–527

Wang ZG, Wan PJ, Ding MM, Yi X, Li JH, Fu Q, Tan H (2011c) Synthesis and micellization of new biodegradable phosphorylcholine-capped polyurethane. J Polym Sci, Part A: Polym Chem 49(9):2033–2042

Wang XH, Guo YZ, Li D, Chen H, Sun RC (2012) Fluorescent amphiphilic cellulose nanoaggregates for sensing trace explosives in aqueous solution. Chem Commun 48(45): 5569–5571

Wei YP, Cheng F (2007) Synthesis and aggregates of cellulose-based hydrophobically associating polymer. Carbohydr Polym 68(4):734–739

Wei H, Zhang XZ, Cheng H, Chen WQ, Cheng SX, Zhuo RX (2006) Self-assembled thermo- and pH-responsive micelles of poly (10-undecenoic acid-b-N-isopropylacrylamide) for drug delivery. J Control Release 116(3):266–274

Winnik FM, Regismond STA (1996) Fluorescence methods in the study of the interactions of surfactants with polymers. Colloids Surf Physicochem Eng Aspects 118(1–2):1–39

Yan CH, Zhang JM, Lv YX, Yu J, Wu J, Zhang J, He JS (2009a) Thermoplastic cellulose-graft-poly (L-lactide) copolymers homogeneously synthesized in an ionic liquid with 4-dimethylaminopyridine catalyst. Biomacromolecules 10(8):2013–2018

Yan Q, Yuan JY, Zhang FB, Sui XF, Xie XM, Yin YW, Wang SF, Wei Y (2009b) Cellulose-based dual graft molecular brushes as potential drug nanocarriers: stimulus-responsive micelles, self-assembled phase transition behavior, and tunable crystalline morphologies. Biomacromolecules 10(8): 2033–2042

Yang LQ, Kuang JL, Wang J, Li ZQ, Zhang LM (2008) Loading and in vitro controlled release of indomethacin using amphiphilic cholesteryl-bearing carboxymethylcellulose derivatives. Macromol Biosci 8(3):279–286

Yu HL, Huang QR (2010) Enhanced in vitro anti-cancer activity of curcumin encapsulated in hydrophobically modified starch. Food Chem 119(2):669–674

Yu X, Zhao ZL, Nie W, Deng RH, Liu SQ, Liang RJ, Zhu JT, Ji XL (2011) Biodegradable polymer microcapsules fabrication through a template-free approach. Langmuir 27(16): 10265–10273

Zhang CY, Yang YQ, Huang TX, Zhao B, Guo XD, Wang JF, Zhang LJ (2012) Self-assembled pH-responsive MPEG-b-(PLA-co-PAE) block copolymer micelles for anticancer drug delivery. Biomaterials 33(26):6273–6283